MOLECULAR AND CELLULAR BIOLOGY, Nov. 2001, p. 7442–7448 Vol. 21, No. 21
0270-7306/01/$04.00+0 DOI: 10.1128/MCB.21.21.7442–7448.2001

Role of β-Dystrobrevin in Nonmuscle Dystrophin-Associated Protein Complex-Like Complexes in Kidney and Liver

NELLIE Y. LOH,[1]† DANIELA NEBENIUS-OOSTHUIZEN,[2]‡ DEREK J. BLAKE,[1]§
ANDREW J. H. SMITH,[2] AND KAY E. DAVIES[1,3]*

MRC Functional Genetics Unit,[3] Department of Human Anatomy and Genetics,[1] University of Oxford, Oxford OX1 3QX, and Centre for Genome Research, The University of Edinburgh, Edinburgh EH9 3JQ,[2] United Kingdom

Received 27 July 2001/Accepted 31 July 2001

β-Dystrobrevin is a dystrophin-related and -associated protein that is highly expressed in brain, kidney, and liver. Recent studies with the kidneys of the *mdx3Cv* mouse, which lacks all dystrophin isoforms, suggest that β-dystrobrevin, and not the dystrophin isoforms, may be the key component in the assembly of complexes similar to the muscle dystrophin-associated protein complexes (DPC) in nonmuscle tissues. To understand the role of β-dystrobrevin in the function of nonmuscle tissues, we generated β-dystrobrevin-deficient (*dtnb*$^{-/-}$) mice by gene targeting. *dtnb*$^{-/-}$ mice are healthy, fertile, and normal in appearance. No β-dystrobrevin was detected in these mice by Western blotting or immunocytochemistry. In addition, the levels of several β-dystrobrevin-interacting proteins, namely Dp71 isoforms and the syntrophins, were greatly reduced from the basal membranes of kidney tubules and liver sinusoids and on Western blots of crude kidney and liver microsomes of β-dystrobrevin-deficient mice. However, no abnormality was detected in the ultrastructure of membranes of kidney and liver cells or in the renal function of these mice. β-Dystrobrevin may therefore be an anchor or scaffold for Dp71 and syntrophin isoforms, as well as other associating proteins at the basal membranes of kidney and liver, but is not necessary for the normal function of these mice.

Dystrobrevins are a group of dystrophin-associated proteins that have significant sequence homology with the cysteine-rich C-terminal region of dystrophin, the product of the X-linked Duchenne muscular dystrophy (DMD) gene. This region of similarity can be divided into several protein-binding domains, namely a ZZ domain, one or two syntrophin binding sites, and two tandem α-helical coiled coils. The syntrophin binding sites mediate interaction with the syntrophins, a family of modular adapter proteins, while the N-terminal α-helical coiled coil binds with the reciprocal region of dystrophin isoforms and utrophin, the autosomal homologue of dystrophin (1, 7, 16, 20).

The dystrobrevin protein family comprises α- and β-dystrobrevin. α-Dystrobrevin is expressed predominantly in skeletal muscle, heart, brain, and lung (4, 19). Differential splicing of the α-dystrobrevin message results in three successively C-terminal-truncated isoforms in skeletal and cardiac muscle (4, 14). In skeletal muscle, α-dystrobrevin is part of a multimolecular dystrophin-associated protein complex (DPC) that connects the actin cytoskeleton and the extracellular matrix (ECM). This bridge is thought to be important for protecting the muscle membrane from stresses incurred during contraction and relaxation. The DPC can be divided into three subcomplexes, namely the membrane-spanning dystroglycan complex, the muscle-specific sarcoglycan complex, and the cytoplasmic complex that comprises α-dystrobrevin, syntrophin, and dystrophin. In DMD muscle, the absence of dystrophin results in muscle degeneration that is coupled with a dramatic reduction of the DPC from the sarcolemma (1). In contrast, targeted disruption of the α-dystrobrevin gene in the mouse leads to mild muscular dystrophy that does not interfere with the assembly of the DPC at the sarcolemma. Since the cytoskeleton-ECM connection is not disrupted, it has been proposed that the muscle degeneration observed in α-dystrobrevin-deficient mice (*adbn*$^{-/-}$ mice) is due to deficiency in intracellular signaling mediated by α-dystrobrevin (9). At the postsynaptic membrane of neuromuscular junctions (NMJs) of skeletal muscle, α-dystrobrevin associates with two complexes: the DPC at the troughs and with utrophin in a complex not unlike the DPC, but at the crests. The NMJs of *abdn*$^{-/-}$ mice mature abnormally, suggesting α-dystrobrevin is required for the maturation of the postsynaptic membrane (10). In brain, α-dystrobrevin-1 is present in the glia and microvasculature (2, 3). The effect of α-dystrobrevin deficiency in this tissue is not known.

β-Dystrobrevin is a dystrophin-associated protein of unknown function that is expressed in a wide variety of nonmuscle tissues, but is found most abundant in brain, kidney, liver, and lung. In brain, β-dystrobrevin associates with dystrophin in hippocampal and Purkinje neurons and is found highly enriched in postsynaptic densities (2, 3). This finding is important, since approximately a third of DMD patients have cognitive impairment. In kidney, β-dystrobrevin is part of several different DPC-like complexes that are localized in a cell-type-specific manner (12). In *mdx3Cv* mice that lack all known

* Corresponding author. Mailing address: Department of Human Anatomy and Genetics, University of Oxford, South Parks Rd., Oxford OX1 3QX, United Kingdom. Phone: (1865) 272179. Fax: (1865) 272420. E-mail: kay.davies@human-anatomy.ox.ac.uk.

† Present address: Nuffield Department of Clinical Medicine, John Radcliffe Hospital, University of Oxford, Oxford OX3 9DU, United Kingdom.

‡ Present address: Deutsches Krcbsforschungszentrum Heidelberg, Abteilung Molekularbiologie der Zelle 1, 69120 Heidelberg, Germany.

§ Present address: Department of Pharmacology, University of Oxford, Oxford OX1 3QT, United Kingdom.

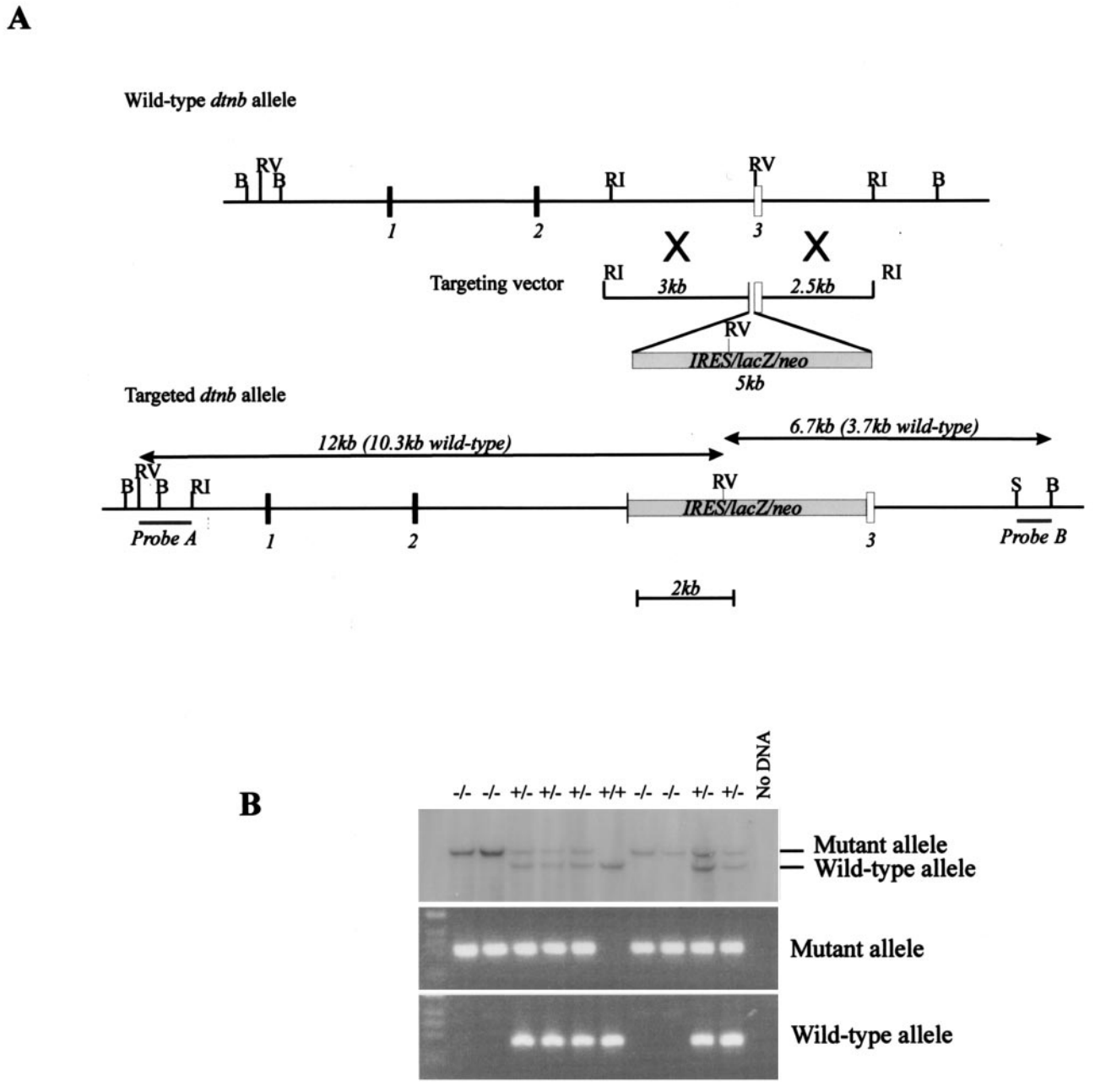

FIG. 1. (A) Targeted inactivation of the mouse β-dystrobrevin gene. Restriction map of the wild-type allele of the *Dtnb* gene, the targeting vector, and the predicted product of homologous recombination. An open box represents the targeted exon. The external probes used for the Southern blot analyses are shown. B, *Bam*HI; RI, *Eco*RI; RV, *Eco*RV; S, *Sac*I. (B) Genotype analyses of offspring from heterozygote matings. The top panel shows a Southern blot of *Eco*RV-digested genomic DNA from tail biopsies probed with a 1.2-kb *Eco*RV-*Eco*RI DNA fragment external to the targeted site (probe A). The wild-type allele produces a ~10.3-kb band, while the mutant allele produces a ~12-kb band. The middle and bottom panels show the products of PCR amplification of the mutant and wild-type alleles, respectively, of the same DNA samples.

dystrophin isoforms, β-dystrobrevin expression and localization at the membrane in brain and kidney are not affected. Thus, it has been speculated that this protein may be the key regulator of DPC-like complex formation and maintenance in nonmuscle tissues (2, 12). The β-dystrobrevin gene (*Dtnb*) has been mapped to the proximal region of mouse chromosome 12 and human chromosome 2p22–23 (11, 18). To date, this gene is not associated with any known genetic disorder. To investigate into the function of the protein, a mouse deficient for the β-dystrobrevin protein was generated by targeted disruption of the *Dtnb* gene.

MATERIALS AND METHODS

Gene targeting construct. An 18-kb genomic fragment containing β-dystrobrevin coding exons 1, 2, and 3 was isolated from a mouse 129/SvJ genomic library in lambda FIX II (Stratagene) by using a 5′-end mouse β-dystrobrevin cDNA clone. A 5.5-kb *Eco*RI fragment comprising exon 3 flanked by 3 and 2.5 kb of intronic sequence upstream and downstream, respectively, was subcloned

into pGEM7Zf(+) (Promega). A $(TAG)_3$/IRES/*lacZ*/SV40pA/MC1*neo*pA (15) cassette was inserted into the *Eco*RV site of the exon. Two hundred micrograms of the targeting construct was linearized with *Xho*I and purified with Geneclean III (BIO 101) prior to electroporation.

Generation of *dtnb*$^{-/-}$ mutant mice. One-hundred-fifty- and 50-μg samples of linearized targeting construct were introduced into 5×10^7 E14-TG2a.IV embryonic stem (ES) cells by electroporation (800 V, 3 μF in phosphate-buffered saline). Recombinant ES cells were selected for G418 resistance. A total of 600 colonies were isolated and cultured in 96-well plates. The correct targeting events were determined by Southern blot analysis of *Bam*HI- and *Eco*RV-digested ES cell DNA with probes 5′ and 3′ to the targeted site (Fig. 1A). Three clones containing the correct targeting event were injected into C57BL/6 blastocysts, which were then transferred into pseudopregnant females. Thirteen chimeras were produced, of which 12 were male, and all were 80 to 90% chimeric by coat color. Four male chimeras from the three clones were bred with C57BL/6 females, and germ-line transmission was determined by Southern blot analysis of DNA from tail biopsies of agouti coat-colored offspring. *dtnb*$^{+/-}$ mice derived from the test crosses were mated to produce *dtnb*$^{-/-}$ offspring at a ratio of 1:4. All mice used in subsequent analyses were over 8 weeks old.

Genotyping. Mice were genotyped by Southern blot or PCR analysis of DNA from tail biopsies. For Southern blot analysis, DNA from tail biopsies was digested with *Eco*RV with or without a second digestion with *Bam*HI, resolved on a 1% agarose gel, and transferred onto Hybond N+ membrane (Amersham Pharmacia). Blots were probed with either a 1.2-kb *Eco*RV-*Eco*RI 5′ probe (probe A) for *Eco*RV-digested DNA or a 0.7-kb *Sac*I-*Bam*HI 3′ probe (probe B) for *Eco*RV-*Bam*HI-digested DNA. PCR analyses of DNA from tail biopsies were performed as follows. The mutant allele was amplified with the IRES T3′ primer (5′GATTCGCAGCGCATCGCCTTC) and the 487R primer (5′TGTC GTAGGCGGCGACCAT), while the wild-type allele was amplified with the 5′Ex3 primer (5′TGTCCAGTTGTGAGGTGACAC) and the 487R primer. Both PCRs were performed under the following cycling conditions: 1 cycle of 94°C for 4 min, 58°C for 2 min, and 72°C for 6 min, followed by 30 cycles of 94°C for 50 s, 58°C for 50 s, and 72°C for 50 s, and then 1 cycle of 94°C for 2 min, 58°C for 2 min, and 72°C for 6 min.

Antibodies. All antibodies mentioned in this paper have been described previously: βCT-FP (anti-β-dystrobrevin and anti-α-dystrobrevin-1 and -2) and α1CT-FP (anti-α-dystrobrevin-1) (3); β521 (anti-β-dystrobrevin), URD40 (antiutrophin), 2166, which was raised against the last 17 amino acids of mouse dystrophin (antidystrophin, Dp71), and 2401, which was raised against the alternatively spliced C terminus of dystrophin (anti-Dp71ΔC) (2); and isoform-specific antisyntrophin antibodies 2688 (anti-α-syntrophin), 2689 (anti-β1-syntrophin), and 2045 (anti-β2-syntrophin) (12). Antiactin antibody was purchased from Sigma-Aldrich (catalog no. A2066).

Western blot analysis. Protein extracts were prepared essentially as described in reference 12. Briefly, fresh frozen tissues were homogenized in treatment buffer (75 mM Tris-HCl [pH 6.8], 4 M urea, 3.8% sodium dodecyl sulfate (SDS), 20% [vol/vol] glycerol, 5% [vol/vol] 2-mercaptoethanol). Twenty micrograms of proteins from each tissue were separated on SDS-polyacrylamide gel electrophoresis (PAGE) gels (8% polyacrylamide) and transferred onto nitrocellulose membranes (Schleicher and Schuell) in transfer buffer (20% ethanol, 0.1% SDS, 192 mM glycine, 25 mM Tris-HCl [pH 8.5]). Membranes were blocked in 5% milk powder in Tris-buffered saline–Tween 20 (TBST; 150 mM NaCl, 50 mM Tris-HCl [pH 7.5], 0.1% Tween 20) for an hour. Blots were incubated for an hour at room temperature with antibodies in 5% milk–TBST solution at the following concentrations: βCT-FP, 1:1,000; α1CT-FP, 1:3,000; URD40, 1:250; 2166, 1:500; or 2401, 1:50. Blots were subsequently washed twice in TBST and twice in 5% milk–TBST for 5 min each. Horseradish peroxidase-conjugated donkey anti-rabbit antibodies (Jackson ImmunoResearch) were applied at 1:3,000 in 5% milk–TBST for 1 h at room temperature after which the membranes were washed four times in TBST. Bound antibodies were detected with a BM chemiluminescence detection kit (Roche).

Microsome preparation and analysis. Crude microsomes from *dtnb*$^{+/+}$ and *dtnb*$^{-/-}$ kidneys and liver were prepared in the following manner. Fresh frozen kidneys and liver were homogenized in 2 or 4 ml of ice-cold microsome buffer containing 300 mM sucrose, 10 mM PIPES [piperazine-*N*, *N*′-bis(2-ethanesulfonic acid)] (pH 6.8), 10 mM NaCl, 3 mM $MgCl_2$, 1 mM EGTA, and protease inhibitors (Complete; Roche). Homogenates were centrifuged at $700 \times g$ for 10 min at 4°C to pellet the nuclear fraction. The postnuclear supernatant was passed through a sieve with pore size of 40 μm (Falcon) and then centrifuged at $141{,}000 \times g$ at 4°C for 45 min with an SW41 Ti rotor (Beckman) to pellet insoluble material. The supernatant was carefully removed, and the pellet was homogenized in half of the original volume of ice-cold microsome buffer. Thirty micrograms of microsomes was separated on SDS-PAGE gels (8% polyacrylamide) and processed for Western blot analysis with the βCT-FP (1:1,000), α1CT-FP (1:3,000), URD40 (1:250), 2166 (1:500), 2401 (1:50), 2689 (1:250), and antiactin (1:500) antibodies.

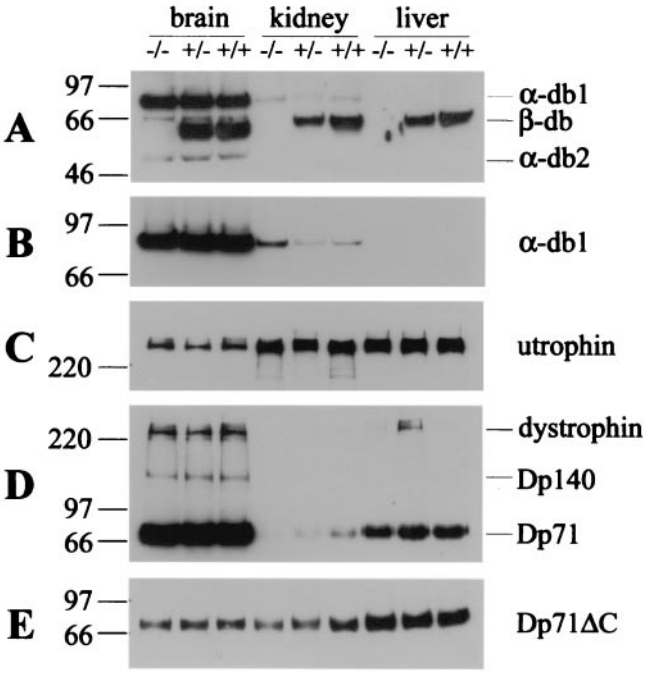

FIG. 2. Western blot analyses. Twenty micrograms (each) of total protein extracts from brain, kidneys, and liver of *dtnb*$^{-/-}$, *dtnb*$^{+/-}$, and *dtnb*$^{+/+}$ littermates was probed with βCT-FP (A), α1CT-FP (B), URD40 (C), 2166 (D), and 2401 (E) antibodies. The proteins that are recognized by these antibodies are shown to the right of the panels, while the positions of protein standards are shown to the left in kilodaltons. db, dystrobrevin.

Immunofluorescence analysis. Ten-micrometer cryosections of kidneys and liver were processed for immunofluorescence labeling as previously described (12). Slides were incubated for 1 h at room temperature in primary antibodies diluted in TBS (150 mM NaCl, 50 mM Tris-HCl [pH 7.5]) at the following dilutions: β521, 1:200; α1CT-FP, 1:250; URD40, 1:250; 2401, 1:20; 2688, 1:50; 2689, 1:200; and 2045, 1:100. This was followed by incubation with rhodamine red-X-conjugated donkey anti-rabbit antibodies (Jackson ImmunoResearch) at a dilution of 1:100. Washed slides were mounted in Vectashield (Vector Laboratories), visualized with a Leica DMRE fluorescence microscope, and photographed with a Leica DMLD camera. For direct comparison of fluorescence intensity, *dtnb*$^{+/+}$ and *dtnb*$^{-/-}$ tissues were photographed under identical settings.

Urine analysis. Spot urine samples were obtained from mice >6 months old and assayed for creatinine, protein, calcium, and glucose levels on the day of sampling. Urine creatinine was measured by using the alkaline picrate colorimetric assay (Sigma-Aldrich). Total protein was measured by using the Bio-Rad protein assay kit. Calcium levels were measured with the calcium-cresolphthalein colorimetric assay (Sigma-Aldrich). Glucose was measured with the Infinity glucose reagent (Sigma-Aldrich). All assays were performed according to the manufacturer's instructions. Urine samples were diluted 1:20 in deionized water for creatinine and protein assays. Ratios of urine protein to creatinine, calcium to creatinine, and glucose to creatinine were used as indices of proteinuria, calciuria, and glucouria, respectively. The data are presented as means ± standard errors. The statistical significance of the difference between mean values of test and control groups was assessed by using the two-tailed Student's *t* test. Differences between mean values of mutant and control groups were considered significant when the *P* value was <0.05.

RESULTS

Generation of *dtnb*$^{-/-}$ mice and their phenotype. The β-dystrobrevin gene spans over 130 kb and comprises at least 21

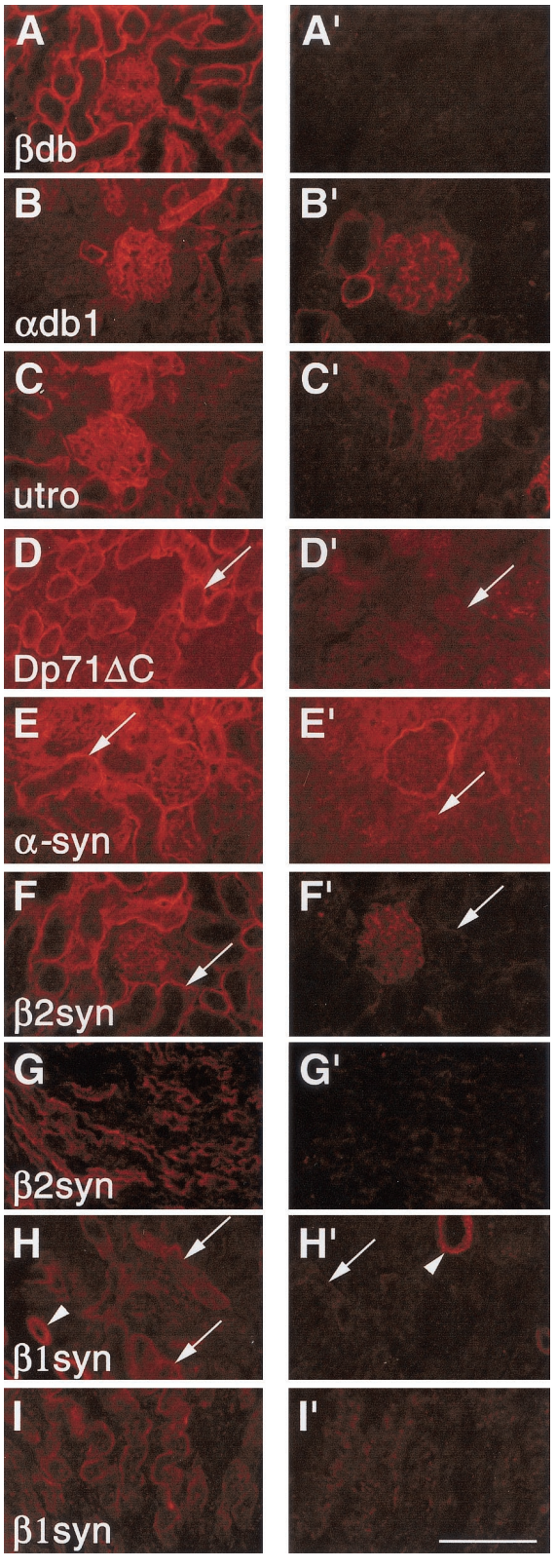

FIG. 3. Immunofluorescence examination of dystrophin-related and -associated proteins in wild-type control (A to I) and *dtnb*$^{-/-}$ (A′ to I′) kidneys. Kidney cryosections were probed with β521 (anti-β-dystrobrevin; A and A′), α1CT-FP (anti-α-dystrobrevin-1; B and B′), URD40 (anti-utrophin; C and C′), 2401 (anti-Dp71ΔC; D and D′), 2688 (anti-α-syntrophin; E and E′), 2045 (anti-β2-syntrophin; F, F′, G, and G′), and 2689 (anti-β1-syntrophin; H, H′, and I, I′). *dtnb*$^{-/-}$ kidneys were prepared and photographed under identical conditions to control kidneys for comparison of fluorescence intensity. Arrows indicate the basal membranes of cortical renal tubules, and arrowheads indicate blood vessels. db, dystrobrevin, utro, utrophin, syn, syntrophin. Bar, 100 μm.

exons, 5 of which are alternatively spliced in a tissue-specific manner. Furthermore, there is evidence that this gene is regulated by at least two promoters (11). To ensure that all known β-dystrobrevin isoforms were disrupted, a $(TAG)_3$/IRES/*lacZ*/SV40pA/MC1*neo*pA (15) cassette was inserted into exon 3, which encodes part of the EF hand region that is present in all known β-dystrobrevin isoforms, to disrupt the reading frame (Fig. 1A). This cassette contains stop codons in three open reading frames at the 5′ end of the internal ribosome entry site (IRES) cassette to ensure that only a truncated form of the β-dystrobrevin protein is produced. The mutation was introduced into ES cells by homologous recombination. Matings between chimeric male mice and C57BL/6 female mice produced heterozygous offspring, indicating that the mutation was transmitted through the germ line. Matings between heterozygous mice produced offspring that were wild type and heterozygous or homozygous for the mutation (Fig. 1B) at a ratio of 1:2:1.

Mice that are heterozygous (*dtnb*$^{+/-}$) and homozygous (*dtnb*$^{-/-}$) for the mutant gene were viable, fertile, and indistinguishable from their wild-type littermates. Histological examination of various tissues by hematoxylin and eosin staining revealed no gross morphological abnormality (data not shown). No β-dystrobrevin was detected in the *dtnb*$^{-/-}$ tissues either on Western blots or by immunofluorescence examination (Fig. 2A, 3A′, and 4A′). Levels of β-dystrobrevin in *dtnb*$^{+/-}$ tissues were reduced by up to half of the levels seen in *dtnb*$^{+/+}$ tissues, showing that in normal tissues, both copies of the gene are active (Fig. 2A). To analyze the effect of β-dystrobrevin loss on the levels of other dystrophin-related proteins and isoforms, Western blot analyses were performed with the same samples with antibodies against α-dystrobrevin-1, utrophin, and two C-terminal splice forms of dystrophin and Dp71. No difference could be detected in the levels of any of the proteins in brain or liver (Fig. 2B to E). However, in *dtnb*$^{-/-}$ kidney, there appeared to be a moderate increase in α-dystrobrevin-1 (Fig. 2B), while levels of Dp71 and Dp71ΔC were noticeably reduced (Fig. 2D and E).

β-Dystrobrevin loss affects the localization of Dp71ΔC and syntrophins at the basal region of cortical renal tubules and liver sinusoids. To analyze the effect of β-dystrobrevin deficiency on the distribution of dystrophin-related and associated proteins, we performed immunofluorescence analyses of *dtnb*$^{+/+}$ and *dtnb*$^{-/-}$ kidneys by using isoform-specific antibodies. In normal kidney, β-dystrobrevin is present in glomeruli, Bowman's capsules, and the basolateral membranes of cortical renal tubules and collecting ducts, whereas α-dystrobrevin-1 is restricted to the glomeruli, blood vessels, and a subset of cortical renal tubules (Fig. 3A and B) (12). As expected no β-dystrobrevin was detected in *dtnb*$^{-/-}$ kidneys (Fig. 3A′). Surprisingly, in light of the increase in the overall level of α-dystrobrevin-1 in *dtnb*$^{-/-}$ kidney, no difference was detected in the localization of α-dystrobrevin-1 in

dtnb$^{-/-}$ kidney by immunofluorescence. Nor was there any obvious increase in overall staining intensity with the α1CT-FP antibody (Fig. 3B′). Thus, the moderate increase in α-dystrobrevin-1 on Western blots of *dtnb*$^{-/-}$ kidney is not due to compensation for the absence of β-dystrobrevin in renal tubules and collecting ducts.

Previously, we showed that β-dystrobrevin colocalizes and coimmunoprecipitates with utrophin, Dp71ΔC, and the syntrophins in normal kidney (12). Here, we found no difference in utrophin staining in control and *dtnb*$^{-/-}$ kidneys (Fig. 3C and C′). In contrast, Dp71ΔC, which is present in the basal regions of normal cortical renal tubules (Fig. 3D), was markedly reduced or undetectable in corresponding regions of *dtnb*$^{-/-}$ kidneys. Similar results were observed with α-syntrophin (Fig. 3E and E′) and β2-syntrophin (Fig. 3F and F′) in this region. In addition, β2-syntrophin staining was lost from collecting ducts (Fig. 3G and G′), but not from glomeruli of *dtnb*$^{-/-}$ kidneys (Fig. 3F and F′). α-Syntrophin staining in collecting ducts was unchanged (data not shown). The persistence of β2-syntrophin at the glomerulus could be due to the presence of α-dystrobrevin-1 or utrophin, while the retention of α-syntrophin in collecting ducts may be due to utrophin or another membrane-associated protein. In normal kidney, β1-syntrophin is found in blood vessels, a subset of cortical renal tubules, and corticomedullary collecting tubules (Fig. 3H and I). In the *dtnb*$^{-/-}$ kidneys, there was a marked decrease in β1-syntrophin staining from the latter two structures, but levels were unaltered in blood vessels (Fig. 3H′ and I′).

To determine if β-dystrobrevin loss had a similar effect on its known ligands in liver, a similar study was conducted with liver cryosections of control and *dtnb*$^{-/-}$ mice. In normal liver, β-dystrobrevin, Dp71ΔC, and β1-syntrophin are localized at the sinusoids and/or at the sinusoidal face of hepatocytes, but not in capillaries or large blood vessels (Fig. 4A, D, and E). Conversely, α-dystrobrevin-1 is found in capillaries and large blood vessels, but not in sinusoids (Fig. 4B), while utrophin is present in both sinusoids and larger blood vessels (Fig. 4C). As expected, β-dystrobrevin was undetectable in *dtnb*$^{-/-}$ liver (Fig. 4A′). Again, distribution of α-dystrobrevin-1 and utrophin was unaltered in *dtnb*$^{-/-}$ liver (Fig. 4B′ and C′). However, no Dp71ΔC staining was detectable at the sinusoids, while the intensity of β1-syntrophin staining was reduced to a third of that seen in control liver (Fig. 4D′ and E′).

β-Dystrobrevin facilitates membrane association of Dp71 isoforms in kidney and liver. To confirm our immunofluorescence findings, we prepared microsomes from kidney and liver of control and *dtnb*$^{-/-}$ mice and analyzed their protein content by Western blotting. As predicted, β-dystrobrevin was detected at high levels in microsomes prepared from kidney and liver of control mice, but not *dtnb*$^{-/-}$ mice (Fig. 5A). In agreement with the immunofluorescence data, no obvious difference was seen in the levels of α-dystrobrevin-1 or utrophin between control and *dtnb*$^{-/-}$ kidney microsomes or the levels of utrophin between control and *dtnb*$^{-/-}$ liver microsomes (Fig. 5B and C). In contrast, there was at least a twofold decrease in the levels of Dp71ΔC and β1-syntrophin in *dtnb*$^{-/-}$ kidney microsomes and in the levels of the Dp71 isoforms and β1-syntrophin in *dtnb*$^{-/-}$ liver microsomes compared with the levels of these proteins in corresponding control tissues (Fig. 5D to F). These findings suggest that the loss of immunofluorescence staining observed in *dtnb*$^{-/-}$ kidney and liver is connected with their disassociation from the membrane. Levels of actin, a protein not known to interact with β-dystrobrevin, were not noticeably different in microsomes of *dtnb*$^{-/-}$ and wild-type tissues (Fig. 5G).

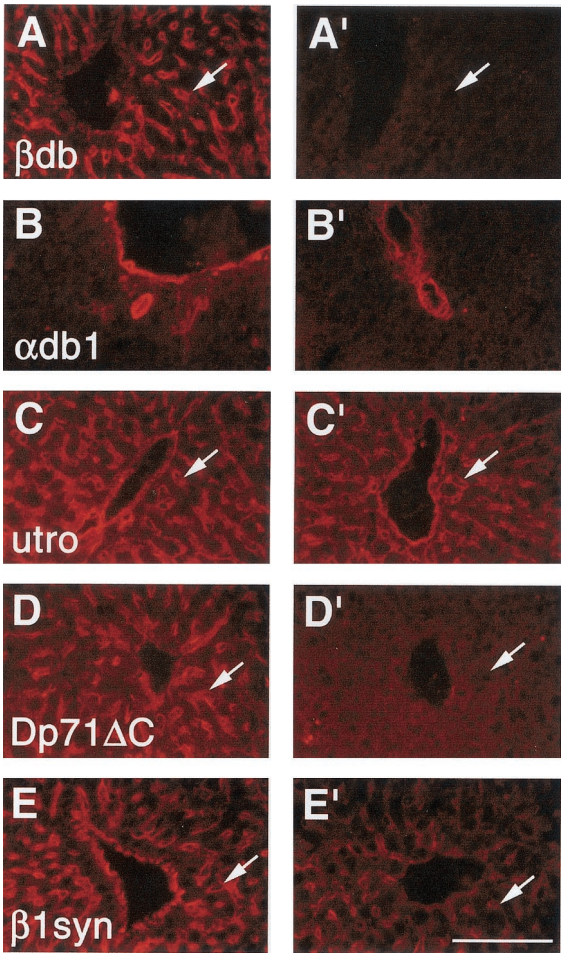

FIG. 4. Immunofluorescence analyses of wild-type control (A to E) and *dtnb*$^{-/-}$ (A′ to E′) liver. Liver cryosections were probed with β521 (anti-β-dystrobrevin; A and A′), α1CT-FP (anti-α-dystrobrevin-1; B and B′), URD40 (anti-utrophin; C and C′), 2401 (anti-Dp71ΔC; D and D′), and 2689 (anti-β1-syntrophin; E and E′) antibodies. *dtnb*$^{-/-}$ livers were prepared and photographed under identical conditions as control liver for comparison of fluorescence intensity. Arrows indicate sinusoids. db, dystrobrevin; utro, utrophin; syn, syntrophin. Bar, 100 μm.

Urine and ultrastructural analyses. To identify possible changes in renal function resulting from this mutation, spot urine samples were obtained from *dtnb*$^{-/-}$ mice and their heterozygous and wild-type littermates and analyzed for abnormal levels of proteinuria, calciuria, and glucouria. The results of our findings are tabulated in Table 1. The differences in protein/creatinine and calcium/creatinine ratios from all groups were not statistically significant. The glucose/creatinine ratios in samples from male and female mice of the *dtnb*$^{+/-}$ and *dtnb*$^{-/-}$ groups were not significantly different. The glucose/creatine value of the samples from female *dtnb*$^{-/-}$ mice was significantly different from that of wild-type females at $P < 0.05$. This could be due to the small sample size, since the differences between glucose/creatinine ratios of wild-type and

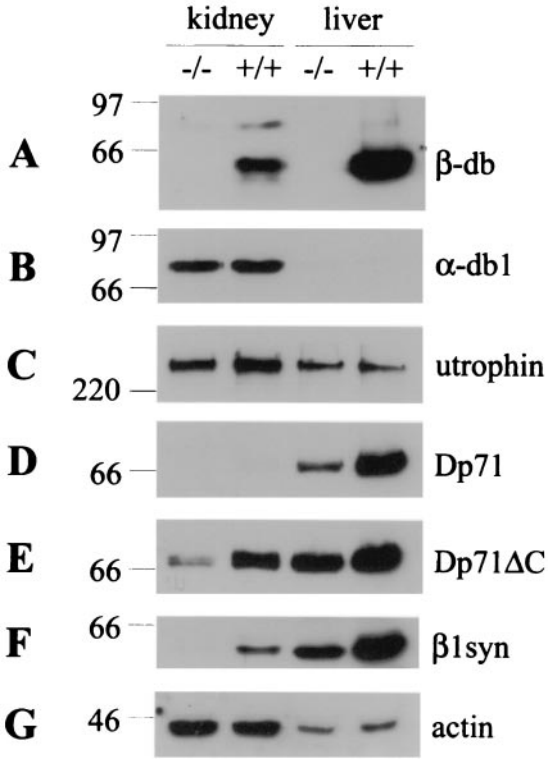

FIG. 5. Western blot analysis of microsomes from control (+/+) and β-dystrobrevin-deficient (−/−) kidneys and liver. Thirty micrograms of microsomes was separated on SDS-PAGE gels (8% polyacrylamide). Blots were probed with the βCT-FP (A), α1CT-FP (B), URD40 (C), 2166 (D), 2401 (E), 2689 (F), and antiactin (G) antibodies. The proteins detected by these antibodies are listed to the right of the panels. The positions of protein standards are shown to the left in kilodaltons. db, dystrobrevin; syn, syntrophin.

dtnb$^{-/-}$ male mice and the differences between the pooled data from male and female mice were found to be not significant ($P > 0.7$ for pooled data).

To determine if the loss of β-dystrobrevin led to ultrastructural changes in kidney and liver cells, *dtnb*$^{-/-}$ and control kidneys and liver were examined by electron microscopy. We could find no obvious difference in the ultrastructure of the basolateral membranes of tubular epithelia and podocyte foot processes in kidney or in the ultrastructural features of the sinusoids or the sinusoidal face of hepatocytes in liver of *dtnb*$^{-/-}$ mice (data not shown).

DISCUSSION

We have generated mice with a targeted mutation in exon 3 of the β-dystrobrevin gene. β-Dystrobrevin was undetectable in tissues from mice that were homozygous for the mutation by Western blotting and immunohistochemistry, confirming that this mutation abolishes all known β-dystrobrevin isoforms. Despite the expression of β-dystrobrevin in many tissues, *dtnb*$^{-/-}$ mice are viable, fertile, and show no obvious histological abnormality. Limited investigation of urine samples has so far revealed no functional significance of this mutation to the kidney. Normal expression of α-dystrobrevin-1 in *dtnb*$^{-/-}$ kidney and liver suggests that α-dystrobrevin-1 is not compensating for the absence of β-dystrobrevin in these tissues.

One similarity between the loss of β-dystrobrevin in kidney and liver and the loss of dystrophin in skeletal muscle is the effect of these molecules on the localization of their ligands. In *mdx* and DMD muscle, the absence of dystrophin leads to secondary loss of DPC from the sarcolemma (8, 13, 17). Similarly, in kidney, the loss of β-dystrobrevin from the basolateral region of epithelial cells of cortical renal tubules and collecting tubules resulted in the loss of Dp71ΔC and all three syntrophin isoforms. Likewise the absence of β-dystrobrevin from liver sinusoids led to the secondary loss of Dp71 isoforms and approximately two-thirds of β1-syntrophin molecules. Therefore the membrane localization of these proteins in kidney and liver requires the presence of β-dystrobrevin. Consistent with this idea, the levels of Dp71 isoforms and β1-syntrophin were reduced in microsome preparations of *dtnb*$^{-/-}$ kidneys and liver compared with those prepared from tissues of control littermates. Since β-dystrobrevin and dystroglycan colocalize in both tissues (6) (Fig. 3A and 4A) and dystrobrevin has been shown to bind to dystroglycan in vitro (5), β-dystrobrevin may serve to link interacting molecules to kidney and liver basement membranes via an interaction with dystroglycan.

The function of β-dystrobrevin-containing protein complexes in kidney and liver is not known. Based on work carried out on the dystrophin complexes in skeletal muscle, we know that α-dystrobrevin may be involved in intracellular signaling, either directly or through its association with the syntrophins (9). Therefore, we speculate that β-dystrobrevin may act as a scaffold for signaling molecules in a similar manner. Syntro-

TABLE 1. Protein/creatinine, calcium/creatinine, and glucose/creatinine ratios of spot urine samples

Mouse group (*n*) and parameter	Mean ± SE amt of protein (mg/mg)
Protein/creatinine ratio	
Male	
+/+ (7)	2.84 ± 0.28
+/− (9)	2.68 ± 0.14
−/− (10)	2.72 ± 0.23
Female	
+/+ (6)	1.37 ± 0.11
+/− (9)	1.45 ± 0.11
−/− (6)	1.46 ± 0.10
Calcium/creatinine ratio	
Male	
+/+ (7)	0.161 ± 0.036
+/− (9)	0.122 ± 0.021
−/− (10)	0.179 ± 0.048
Female	
+/+ (6)	0.114 ± 0.051
+/− (9)	0.081 ± 0.016
−/− (6)	0.079 ± 0.015
Glucose/creatinine ratio	
Male	
+/+ (7)	0.779 ± 0.036
+/− (9)	0.707 ± 0.050
−/− (10)	0.703 ± 0.051
Female	
+/+ (6)	0.642 ± 0.030
+/− (9)	0.700 ± 0.032
−/− (6)	0.734 ± 0.029[a]

[a] $P < 0.05$ for same-gender wild-type control versus *dtnb*$^{-/-}$.

phins recruit a variety of signaling molecules to the DPC via binding to their PDZ domains. Recently, we showed that the dystrobrevins, the dystrophin isoforms, and utrophin each contain two tandem syntrophin binding motifs (16). Thus the loss of β-dystrobrevin and Dp71ΔC and the corresponding loss of the syntrophins from the basal membranes of *dtnb*$^{-/-}$ renal tubules and liver suggest that potentially up to four syntrophin-binding signaling molecules per DPC-like complex fail to be recruited to the membrane. Despite its expression in many nonmuscle tissues and its effect on its ligands in kidney and liver, the normal appearance of the *dtnb*$^{-/-}$ mice suggests that β-dystrobrevin is not important for the viability of the mouse. An alternative explanation is that, under normal physiological conditions, the effect of β-dystrobrevin loss is masked, and the true effect of this loss will only become evident when the renal or hepatic system of these mice is challenged.

In conclusion, we have shown that β-dystrobrevin is required for the assembly of Dp71 and syntrophin molecules to the basal membrane of kidney cells and liver sinusoids, but its presence is not critical for the survival of β-dystrobrevin-null mice.

ACKNOWLEDGMENTS

This work was funded by the Wellcome Trust. D.J.B. is a Wellcome Trust Senior Research Fellow.

We thank Sarah Squire, Allyson Potter, Adrian Isaacs, Mohan Masih, Lynne Scott, Karo Tanaka, and Nicholas Owen for advice and technical expertise.

REFERENCES

1. **Blake, D. J., and K. E. Davies.** 1997. Dystrophin and the molecular genetics of muscular dystrophy, p. 219–241. *In* Y. H. Edwards and D. M. Swallow (ed.), Protein dysfunction in human genetic diseases. BIOS Scientific, Oxford, United Kingdom.
2. **Blake, D. J., R. Hawkes, M. A. Benson, and P. W. Beesley.** 1999. Different dystrophin-like complexes are expressed in neurons and glia. J. Cell Biol. **147:**645–658.
3. **Blake, D. J., R. Nawrotzki, N. Y. Loh, D. C. Gorecki, and K. E. Davies.** 1998. Beta-dystrobrevin, a member of the dystrophin-related protein family. Proc. Natl. Acad. Sci. USA **95:**241–246.
4. **Blake, D. J., R. Nawrotzki, M. F. Peters, S. C. Froehner, and K. E. Davies.** 1996. Isoform diversity of dystrobrevin, the murine 87-kDa postsynaptic protein. J. Biol. Chem. **271:**7802–7810.
5. **Chung, W., and J. T. Campanelli.** 1999. WW and EF hand domains of dystrophin-family proteins mediate dystroglycan binding. Mol. Cell Biol. Res. Commun. **2:**162–171.
6. **Durbeej, M., M. D. Henry, M. Ferletta, K. P. Campbell, and P. Ekblom.** 1998. Distribution of dystroglycan in normal adult mouse tissues. J. Histochem. Cytochem. **46:**449–457.
7. **Dwyer, T. M., and S. C. Froehner.** 1995. Direct binding of Torpedo syntrophin to dystrophin and the 87 kDa dystrophin homologue. FEBS Lett. **375:** 91–94.
8. **Ervasti, J. M., K. Ohlendieck, S. D. Kahl, M. G. Gaver, and K. P. Campbell.** 1990. Deficiency of a glycoprotein component of the dystrophin complex in dystrophic muscle. Nature **345:**315–319.
9. **Grady, R. M., R. W. Grange, K. S. Lau, M. M. Maimone, M. C. Nichol, J. T. Stull, and J. R. Sanes.** 1999. Role for alpha-dystrobrevin in the pathogenesis of dystrophin-dependent muscular dystrophies. Nat. Cell Biol. **1:**215–220.
10. **Grady, R. M., H. Zhou, J. M. Cunningham, M. D. Henry, K. P. Campbell, and J. R. Sanes.** 2000. Maturation and maintenance of the neuromuscular synapse: genetic evidence for roles of the dystrophin-glycoprotein complex. Neuron **25:**279–293.
11. **Loh, N. Y., H. J. Ambrose, L. M. Guay-Woodford, S. DasGupta, R. A. Nawrotzki, D. J. Blake, and K. E. Davies.** 1998. Genomic organization and refined mapping of the mouse beta-dystrobrevin gene. Mamm. Genome **9:** 857–862.
12. **Loh, N. Y., S. E. Newey, K. E. Davies, and D. J. Blake.** 2000. Assembly of multiple dystrobrevin-containing complexes in the kidney. J. Cell Sci. **113:** 2715–2724.
13. **Matsumura, K., F. M. Tome, V. Ionasescu, J. M. Ervasti, R. D. Anderson, N. B. Romero, D. Simon, D. Recan, J. C. Kaplan, and M. Fardeau et al.** 1993. Deficiency of dystrophin-associated proteins in Duchenne muscular dystrophy patients lacking COOH-terminal domains of dystrophin. J. Clin. Investig. **92:**866–871.
14. **Nawrotzki, R., N. Y. Loh, M. A. Ruegg, K. E. Davies, and D. J. Blake.** 1998. Characterisation of alpha-dystrobrevin in muscle. J. Cell Sci. **111:**2595–2605.
15. **Nehls, M., B. Kyewski, M. Messerle, R. Waldschutz, K. Schuddekopf, A. J. Smith, and T. Boehm.** 1996. Two genetically separable steps in the differentiation of thymic epithelium. Science **272:**886–889.
16. **Newey, S. E., M. A. Benson, C. P. Ponting, K. E. Davies, and D. J. Blake.** 2000. Alternative splicing of dystrobrevin regulates the stoichiometry of syntrophin binding to the dystrophin protein complex. Curr. Biol. **10:**1295–1298.
17. **Ohlendieck, K., and K. P. Campbell.** 1991. Dystrophin-associated proteins are greatly reduced in skeletal muscle from mdx mice. J. Cell Biol. **115:** 1685–1694.
18. **Peters, M. F., K. F. O'Brien, H. M. Sadoulet-Puccio, L. M. Kunkel, M. E. Adams, and S. C. Froehner.** 1997. Beta-dystrobrevin, a new member of the dystrophin family. Identification, cloning, and protein associations. J. Biol. Chem. **272:**31561–31569.
19. **Sadoulet-Puccio, H. M., T. S. Khurana, J. B. Cohen, and L. M. Kunkel.** 1996. Cloning and characterization of the human homologue of a dystrophin related phosphoprotein found at the Torpedo electric organ post-synaptic membrane. Hum. Mol. Genet. **5:**489–496.
20. **Sadoulet-Puccio, H. M., M. Rajala, and L. M. Kunkel.** 1997. Dystrobrevin and dystrophin: an interaction through coiled-coil motifs. Proc. Natl. Acad. Sci. USA **94:**12413–12418.